RAPID COMMUNICATIONS

https://doi.org/10.1590/2317-4889202320230042

BJGEO Brazilian Journal of Geology

Motion maps derived from optical satellite images: the case study of the East Anatolian Fault (Türkiye)

Marcos Eduardo Hartwig[1]*, Cícero Dias Bottacin[1], Carlos Henrique Grohmann[2]

Abstract

On February 6, 2023, two earthquakes shook the southern and central Türkiye causing significant loss of human life and devastating many cities. These are related to the active East Anatolian Fault (EAF). In this study, the digital image correlation (DIC) technique is applied to map the coseismic displacements. For that, a pair of scenes from the Sentinel-2 satellite acquired before and after the seismic events was used. The results showed that the methodological approach can be effectively used to map and monitor large-scale geological phenomena and can assist in seismic risk assessment.

KEYWORDS: digital image correlation; neotectonics; remote sensing; deformation; structural geology.

INTRODUCTION

Digital image correlation (DIC) is a technique that allows us to detect and monitor horizontal displacements in the plane of digital images (Delacourt *et al.* 2007). It has been successfully used in studies involving landslides, glaciers, active faults, and volcanic eruptions (Hartwig in press; Lucieer *et al.* 2014; Caporossi *et al.* 2018; Morelan and Hernandez 2020).

DIC makes use of digital images acquired by different platforms such as terrestrial fixed cameras, aerial (RPA or aircraft), or orbital (satellites). Furthermore, large horizontal displacements (several meters) can be detected and different image types can be employed (e.g., optics, radar, and digital elevation model). Finally, satellite imagery with global coverage and algorithms for image correlation is now freely available (Leprince *et al.* 2007).

On February 6, 2023, two major earthquakes with magnitudes M_W 7.8 (*Kahramanmaraş* Earthquake) and 7.5 (*Elbistan* Earthquake) followed by several small-intensity seismic events struck southern and central Türkiye (USGS, 2023). These aused thousands of fatalities and surface displacements of a few meters (Karabulut *et al.* 2023; Li *et al.* 2023).

The study area is located in a seismotectonic region (Fig. 1), which has been active since the Early Pliocene due to the convergence among the African, Arabian, and Anatolian tectonic plates (Mckenzie, 1972; Barka and Kadinsky-Cade, 1988; Barka and Reilinger, 1997). The earthquake source mechanism is attributed to the East Anatolian Fault (EAF), which is a 700-km-long left-lateral strike-slip fault (Okay 2008; Duman and Emre 2013).

The aim of this study was to test the DIC technique with optical images of the Sentinel-2 satellite in order to map the surface displacement field produced by the seismic events that struck Türkiye. In addition, the study sought to evaluate possible differences in the displacement maps generated from the visible and near-infrared spectral bands.

Methods and dataset

For a pair of images acquired over the same area to be correlated, it is necessary that they share a common geometry (Delacourt *et al.* 2004). This can be obtained through orthorectification based on a digital elevation model. To

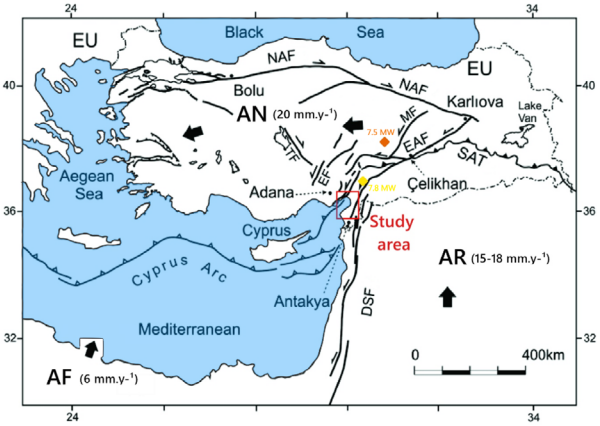

AN: Anatolian plate; AF: African plate; AR: Arabic plate; EU: Eurasian plate; NAF: North Anatolian Fault; EAF: East Anatolian Fault; DSF: Dead Sea Fault; SAT: Southeast Anatolian Thrust Zone; MF: Malatya fault, TF: Tuzgo¨lu¨ fault; EF: Ecemis fault.

Source: after Taymaz *et al.* (2007); Duman and Emre (2013); Karabacak and Altunel (2013); Tari *et al.* (2013); and Aktuğ *et al.* (2016).

Figure 1. Tectonic map of Türkiye and surroundings.

[1]Universidade Federal do Espírito Santo, Department of Geology – Alegre (ES), Brazil. E-mails: marcos.hartwig@ufes.br, cicero.botacin@edu.ufes.br

[2]Universidade de São Paulo, Institute of Energy and Environment – São Paulo (SP), Brazil. E-mail: guano@usp.br

*Corresponding author.

determine offsets, a moving correlation window with a predetermined size is defined over the pre-event image. An equivalent window in the post-event image is searched through correlation functions. The displacement vector is determined when the maximum correlation between the windows is found.

The size of the correlation window affects the displacement accuracy. Larger windows reduce the displacement accuracy. Displacement accuracy that equals one-fifth of the pixel size is typical for satellite images. Displacements of up to 80 pixels have been detected by Delacourt *et al.* (2004) with the DIC technique. Factors such as illumination conditions, surface state, image noise, and radiometric differences between the image pair can affect displacement calculations (Travelletti *et al.* 2012).

Two scenes from the Sentinel-2 satellite acquired on January 25, 2023 and February 09, 2023 were used. Images with processing level 2A (orthorectified) with 10 m of spatial resolution in the visible (B2, B3, and B4 bands) and near-infrared (B8 band) were selected. These are freely available in Copernicus Sentinel Data (2023). Details about the Sentinel-2 satellite and products can be found on ESA (2023).

The COSI-Corr algorithm (Leprince *et al.* 2007) implemented in IDL was chosen for image correlation. The frequency-based correlator was used, and different window sizes were tested. The best result was obtained for a subset of 128 × 128 pixels (1,280 × 1,280 m). E-W and N-S displacement maps were generated. Positive values indicate eastward and northward movement and negative values are the opposite. The signal-to-noise ratio (SNR) map has also been produced. Values close to 1 mean good quality and values close to 0 mean poor quality. Finally, the displacement vectors were calculated based on the N-S and E-W displacement fields. The longer the arrows, the greater the displacement. Movement is indicated by the orientation of the arrows.

The products were then draped over a shaded relief map based on the SRTM-30 m digital elevation model available in USGS EarthExplorer (2023). The illuminant was positioned at azimuth N315° with a solar elevation angle of 45°. Georeferenced structural data from the Geological Institute of the Russian Academy of Sciences available in AFEAD (2023) were used to help interpret the results.

Due to the lack of field validation data, displacement measurements were compared with other studies to verify the consistency of the results.

The *datum* WGS-84 (Zone 36S) and the UTM coordinate system have been adopted.

RESULTS AND DISCUSSION

Figures 2–4 depict the E-W, N-S, and SNR maps for spectral bands 2, 3, 4, and 8.

The Gulf of Alexandretta appears noisy on all maps due to the low correlation between the pairs of images. No significant

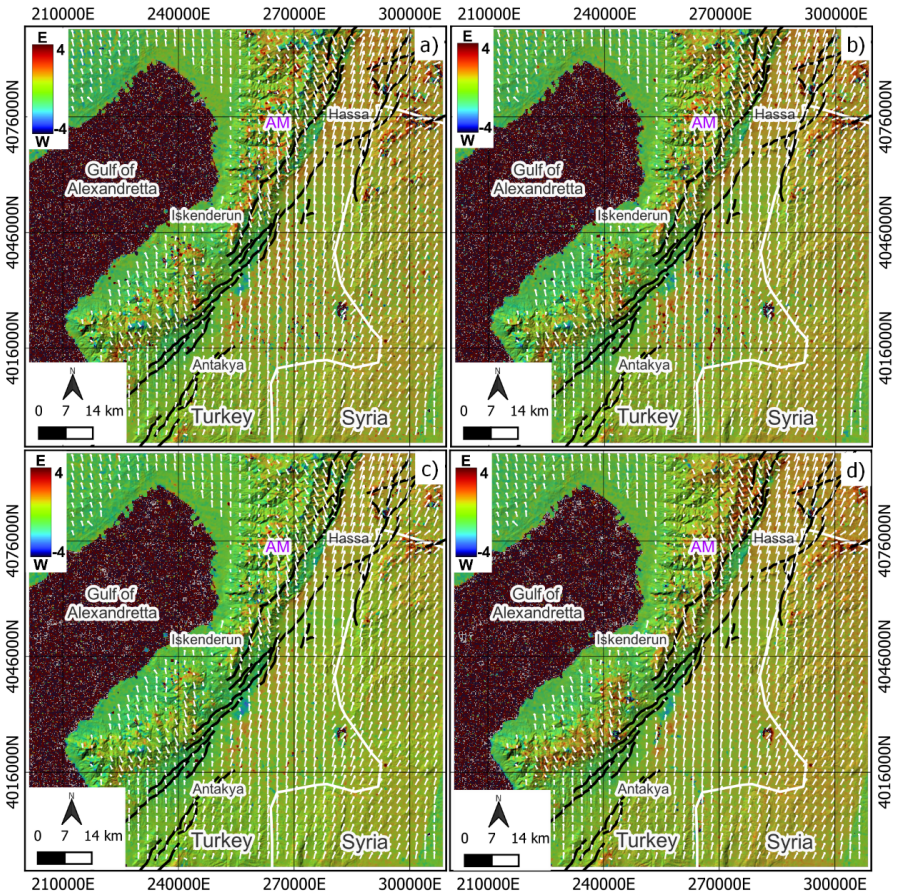

AM: Amanos Mountains.

Figure 2. E-W displacement maps generated using the DIC technique for spectral bands (A) 2, (B) 3, (C) 4, and (D) 8. Solid black lines represent the East Anatolian Fault. The arrows indicate the relative displacement vectors. Displacements are measured in meters.

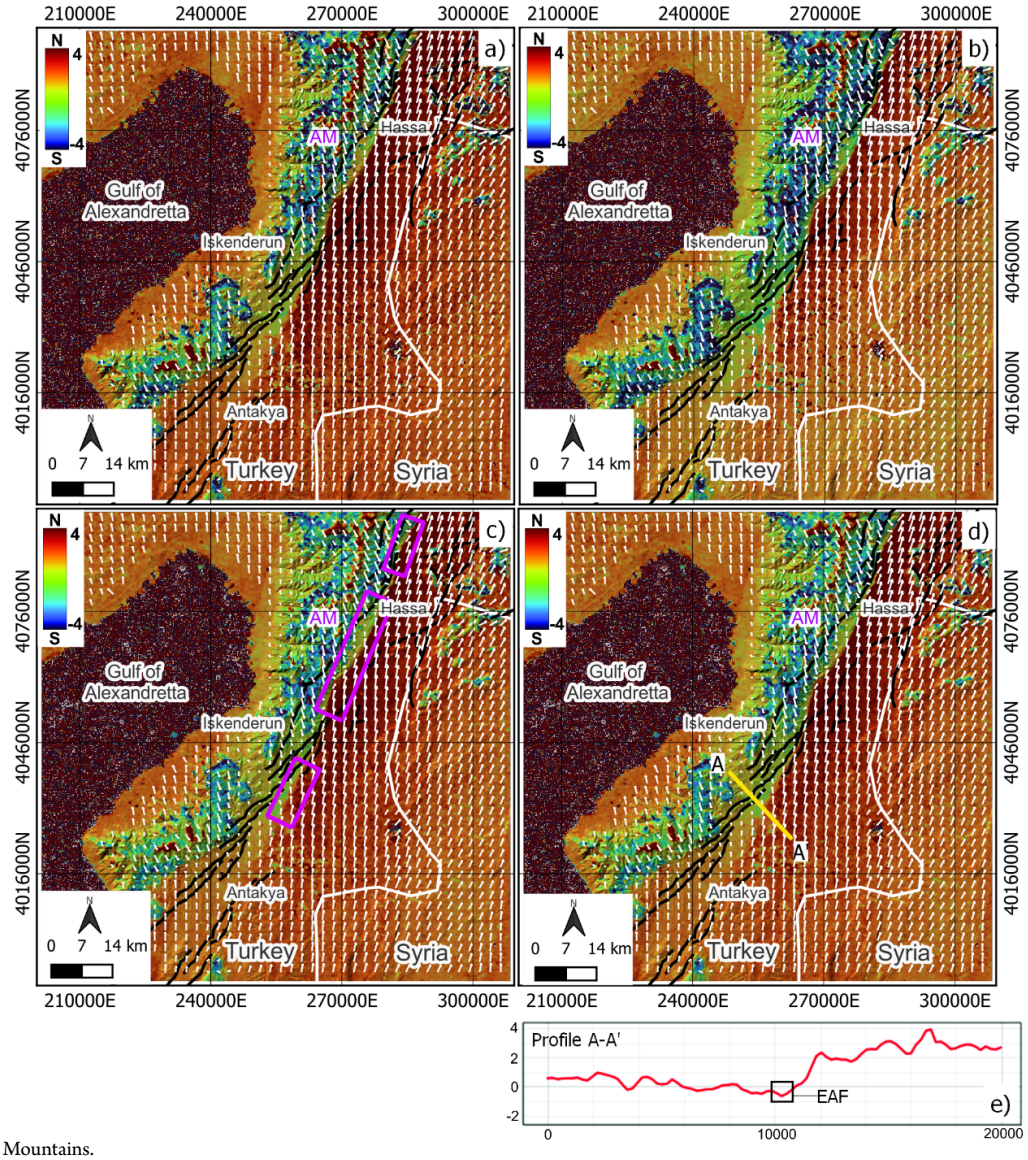

AM: Amanos Mountains.

Figure 3. N-S displacement maps generated using the DIC technique for spectral bands (A) 2, (B) 3, (C) 4, and 8 (D) 8. (E) A-A´ displacement profile. Black solid lines represent the East Anatolian Fault. The arrows indicate the relative displacement vectors, and rectangles indicate regions with new cracks. Displacements are measured in meters.

differences are observed between the maps produced by the four spectral bands.

The peak surface offset is about 5 m. The E-W displacement maps show a subtle hue contrast that coincides with the EAF. For the N-S displacement maps, a sharp hue contrast is visible, showing that the component of displacement in the N-S direction is larger than in the E-W direction. Besides, data clearly show a left-lateral strike-slip motion (Duman and Emre, 2013). Finally, the N-S displacements are larger near the EAF, declining in the east-west direction.

The EAF is made of a series of long parallel lineaments. Figure 3 shows that the fissure created by the seismic events had not been previously mapped. This can be easily recognized by considering the color distribution pattern (contrast between the shades of green and blue versus red). Figure 3e shows a displacement profile that traverses the new fissure. This means that the DIC is capable of tracking active faults and can assist in land use planning.

The SNR maps display most values close to unity, indicating good quality. This is mostly due to the sparse vegetation (i.e., grass and shrubs) that covers the land.

Li et al. (2023) used the pixel offset tracking combined with the weighted least squares technique from radar images of the Sentinel-1 satellite, acquired in ascending and descending orbit tracks, to derive the E-W and N-S displacements caused by the earthquakes that hit the Kahramanmaraş region (Türkiye) on February 06. The magnitude and spatial distribution of the horizontal displacements mapped by the authors are quite similar to the results presented here, even though the method and data used are completely different.

CONCLUSION

The results allow us to conclude the following:

- The DIC technique based on Sentinel-2 images is quite suitable for the detection and monitoring of large-scale geological phenomena;

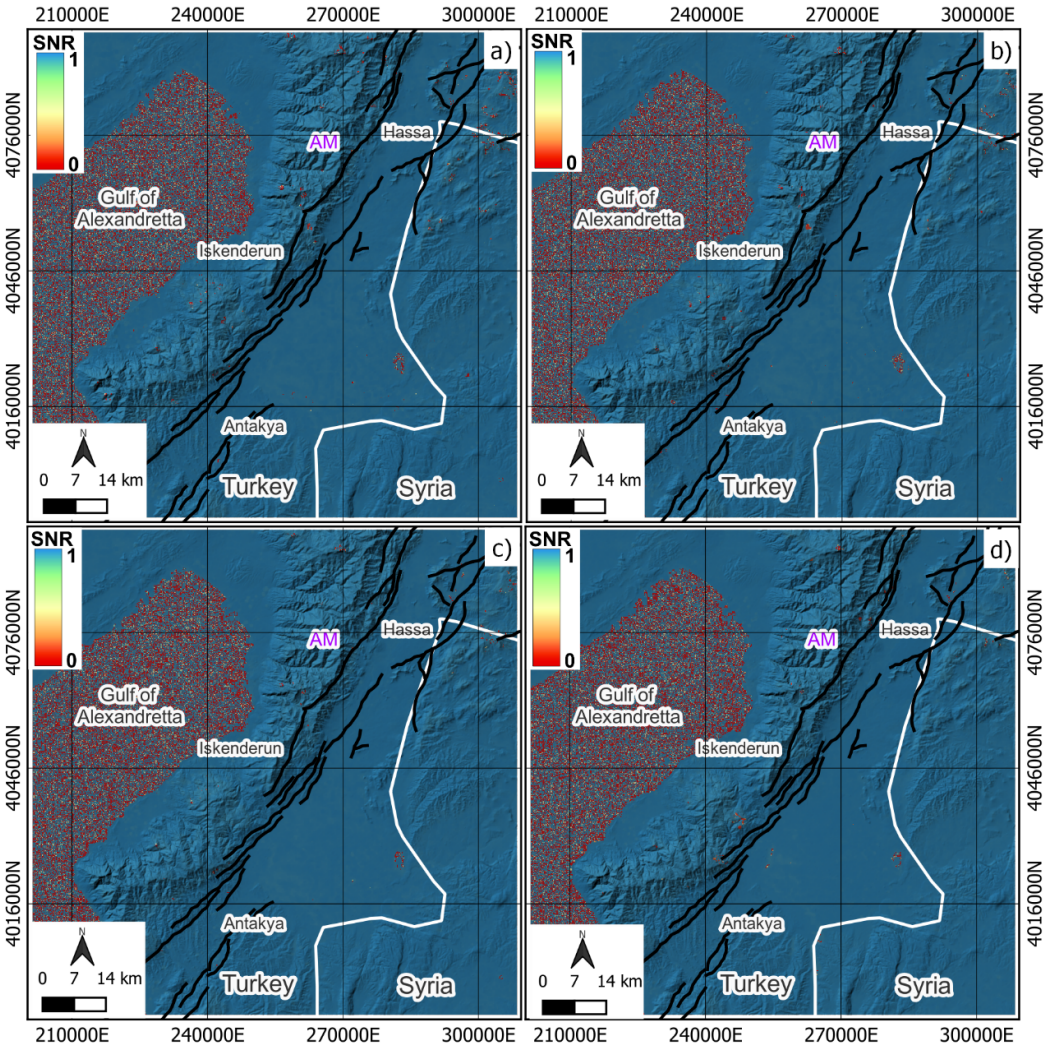

AM: Amanos Mountains.

Figure 4. SNR maps for spectral bands (A) 2, (B) 3, (C) 4, and (D) 8. Black solid lines represent the East Anatolian Fault.

- No significant differences were observed in the displacement maps generated from spectral bands 2, 3, 4, and 8, which reveals that they can be used interchangeably for displacement mapping using DIC;
- The displacement values are consistent with those obtained through other monitoring techniques;
- Displacement data show that the EAF is a sinistral strike-slip fault related to transtensional deformation;
- Finally, the results allowed extrapolating the EAF to areas where it had not yet been mapped, which shows that the DIC can be used to map active geological faults and assist studies on seismic hazards.

ARTICLE INFORMATION

Manuscript ID: 20230042. Received on: 15 AUG 2023. Approved on: 23 OCT 2023.

How to cite: Hartwig M.E., Bottacin C.D., Grohmann C.H. (2023). Motion maps derived from optical satellite images: the case study of the East Anatolian Fault (Türkiye). *Brazilian Journal of Geology*, **53**(3), e20230042. https://doi.org/10.1590/2317-4889202320230042

M.E.H.: Conceptualization, methodology, formal analysis, project administration, supervision, validation, writing – original draft, writing – review & editing. C.D.B.: investigation, visualization, writing – original draft. C.H.G.: writing – review & editing.

Competing interests: The authors declare no competing interests.

REFERENCES

Active Faults of Eurasia Database (AFEAD). 2023. Available at: http://neotec.ginras.ru/index/mapbox/database_map.html. Accessed on: Jul 14, 2023.

Aktuğ B., Özener H., Doğru A., Sabuncu A., Turgut B., Halicioğlu K., Yilmaz O. 2016. Slip rates and seismic potential on the East Anatolian Fault System using an improved GPS velocity field. *Journal of Geodynamics*, 94-95:1-12. https://doi.org/10.1016/j.jog.2016.01.001

Barka A., Reilinger R. 1997. Active tectonics of the Eastern Mediterranean region deduced from GPS, neotectonic and seismicity data. *Annals of Geophysics*, 40(3):587-610. https://doi.org/10.4401/ag-3892

Barka A.A., Kadinsky-Cade K. 1988. Strike-slip fault geometry in Türkiye and its influence on earthquake activity. *Tectonics*, 7(3):663-684. https://doi.org/10.1029/TC007i003p00663

Caporossi P., Mazzanti P., Bozzano F. 2018. Digital image correlation (DIC) analysis of the 3 December 2013 Montescaglioso Landslide (Basilicata, Southern Italy): results from a multi-dataset investigation. *ISPRS International Journal of Geo-Information*, 7(9):372. https://doi.org/10.3390/ijgi7090372

Copernicus Sentinel Data. 2023. Available at: https://scihub.copernicus.eu/dhus/#/home. Accessed on: Jul 14, 2023.

Delacourt C., Allemand P., Berthier E., Raucoules D., Casson B., Grandjean P., Pambrun C., Varel E. 2007. Remote-sensing techniques for analysing landslide kinematics: a review. *Bulletin de Société Géologique*, 178(2):89-100. https://doi.org/10.2113/gssgfbull.178.2.89

Delacourt C., Allemand P., Casson B., Vadon H. 2004. Velocity field of the "La Clapière" landslide measured by the correlation of aerial and QuickBird satellite images. *Geophysical Research Letters*, 31(15):L15619. https://doi.org/10.1029/2004GL020193

Duman T.Y., Emre Ö. 2013. The East Anatolian Fault: geometry, segmentation and jog characteristics. *Geological Society, London, Special Publications*, 372(1):495-529. https://doi.org/10.1144/SP372.14

European Space Agency (ESA). 2023. Sentinel Online. *Sentinel-2 Mission Guide*. Available at: https://sentinel.esa.int/web/sentinel/missions/sentinel-2. Accessed on: March 22, 2023.

Hartwig M.E. Motion maps of glacier Viedma using DIC. *Revista de la Asociación Geológica Argentina*, 80(3). in press.

Karabacak V., Altunel E. 2013. Evolution of the northern Dead Sea fault zone in Southern Türkiye. *Journal of Geodynamics*, 65:282-291. https://doi.org/10.1016/j.jog.2012.04.012

Karabulut H., Güvercin S.E., Hollingsworth J., Konca A.Ö. 2023. Long silence on the East Anatolian Fault Zone (Southern Türkiye) ends with devastating double earthquakes (6 February 2023) over a seismic gap: implications for the seismic potential in the Eastern Mediterranean region. *Journal of the Geological Society*, 180(3):jgs2023-021. https://doi.org/10.1144/jgs2023-021

Leprince S., Barbot S., Ayoub F., Avouac J.P. 2007. Automatic and precise orthorectification, coregistration, and subpixel correlation of satellite images, application to ground deformation measurements. *IEEE Transactions on Geoscience and Remote Sensing*, 45(6):1529-1558. https://doi.org/10.1109/TGRS.2006.888937

Li S., Wang X., Tao T., Zhu Y., Qu X., Li Z., Huang J., Song S. 2023. Source Model of the 2023 Türkiye Earthquake Sequence Imaged by Sentinel-1 and GPS Measurements: Implications for Heterogeneous Fault Behavior along the East Anatolian Fault Zone. *Remote Sensing*, 15(10):2618. https://doi.org/10.3390/rs15102618

Lucieer A., Jong S.M., Turner D. 2014. Mapping landslide displacements using Structure from Motion (SfM) and image correlation of multi-temporal UAV photography. *Progress in Physical Geography: Earth and Environment*, 38(1):97-116. https://doi.org/10.1177/0309133313515293

Mckenzie D. 1972. Active tectonics of the Mediterranean region. *Geophysical Journal International*, 30(2):109-185. https://doi.org/10.1111/j.1365-246X.1972.tb02351.x

Morelan A.E., Hernandez J.L. 2020. Increasing Postearthquake Field Mapping Efficiency with Optical Image Correlation. *Bulletin of the Seismological Society of America*, 110(4):1419-1426. https://doi.org/10.1785/0120200034

Okay A.I. 2008. Geology of Türkiye: a synopsis. *Anschnitt*, 21:19-42.

Tari U., Tüysüz O., Genç Ş.C., İmren C., Blacwell B.A.B., Lom N., Tekeşin Ö., Üsküplü S., Erel L., Atiok S., Beyhan M. 2013. The geology and morphology of the Antakya Graben between the Amik Triple Junction and the Cyprus Arc. *Geodinamica Acta*, 26(1-2):27-55. https://doi.org/10.1080/09853111.2013.858962

Taymaz T., Yilmaz Y., Dilek Y. 2007. The geodynamics of the Aegean and Anatolia: introduction. *Geological Society, London, Special Publications*, 291(1):1-16. https://doi.org/10.1144/SP291.1

Travelletti J., Delacourt C., Allemand P., Malet J.P., Schmittbuhl J., Toussaint R., Bastard M. 2012. Correlation of multi-temporal ground-based optical images for landslide monitoring: Application, potential and limitations. *ISPRS Journal of Photogrammetry and Remote Sensing*, 70:39-55. https://doi.org/10.1016/j.isprsjprs.2012.03.007

United States Geological Survey (USGS). *Earthquake Catalog*. USGS, 2023. Available at: https://earthquake.usgs.gov/earthquakes. Accessed on: March 20, 2023.

United States Geological Survey (USGS) EarthExplorer. 2023. Available at: https://earthexplorer.usgs.gov/. Accessed on: July 14, 2023.